

Reanalysis of lattice QCD spectra leading to the $D_{s0}^*(2317)$ and $D_{s1}^*(2460)$

A. Martínez Torres,^a E. Oset,^b S. Prelovsek^c and A. Ramos^d

^a*Instituto de Física, Universidade de São Paulo,
C.P. 66318, 05389-970 São Paulo, SP, Brazil*

^b*Departamento de Física Teórica and IFIC,
Centro Mixto Universidad de Valencia-CSIC Institutos de Investigación de Paterna,
Aptdo. 22085, 46071 Valencia, Spain*

^c*Department of Physics at University of Ljubljana, Jozef Stefan Institute,
1000 Ljubljana, Slovenia.*

^d*Departament d'Estructura i Constituents de la Matèria and Institut de Ciències del Cosmos,
Universitat de Barcelona, Martí i Franquès 1, E-08028 Barcelona, Spain*

*E-mail: amartine@if.usp.br, Eulogio.Oset@ific.uv.es,
sasa.prelovsek@ijs.si, ramos@ecm.ub.edu*

ABSTRACT: We perform a reanalysis of the energy levels obtained in a recent lattice QCD simulation, from where the existence of bound states of KD and KD^* are induced and identified with the narrow $D_{s0}^*(2317)$ and $D_{s1}^*(2460)$ resonances. The reanalysis is done in terms of an auxiliary potential, employing a single-channel basis $KD^{(*)}$, and a two-channel basis $KD^{(*)}, \eta D_s^{(*)}$. By means of an extended Lüscher method we determine poles of the continuum t -matrix, bound by about 40 MeV with respect to the KD and KD^* thresholds, which we identify with the $D_{s0}^*(2317)$ and $D_{s1}^*(2460)$ resonances. Using a sum rule that reformulates Weinberg compositeness condition we can determine that the state $D_{s0}^*(2317)$ contains a KD component in an amount of about 70%, while the state $D_{s1}^*(2460)$ contains a similar amount of KD^* . We argue that the present lattice simulation results do not still allow us to determine which are the missing channels in the bound state wave functions and we discuss the necessary information that can lead to answer this question.

KEYWORDS: Lattice QCD, Phenomenological Models, QCD

ARXIV EPRINT: [1412.1706](https://arxiv.org/abs/1412.1706)

Contents

1	Introduction	1
2	Compositeness of states	3
3	Analysis of the lattice spectra	6
3.1	Analysis by means of the effective range formula	6
3.2	Analysis of lattice spectra by means of an auxiliary potential	8
3.3	Fit with a CDD pole	10
3.4	Two channel analysis	11
4	Scattering length and effective range	12
5	Evaluation of systematic uncertainties	13
6	Conclusions	17

1 Introduction

The scalar $D_{s0}^*(2317)$ and axial $D_{s1}(2460)$ mesons were experimentally found slightly below KD and KD^* thresholds [1–4]. These are one of the few shallow bound states in the meson sector, and therefore deserve special attention. The effect of thresholds was recently considered using lattice QCD for the first time in this system in [5, 6], where interpolators of KD and KD^* type have been employed in addition to $\bar{s}c$ ones. The $N_f=2+1$ simulation obtained three energy levels for $m_\pi \simeq 156$ MeV in the KD and KD^* systems. The fact that these levels appear clean with the KD and KD^* interpolators, together with the observation that the lowest one appears below and not far from the corresponding KD or KD^* threshold, hint to a possible molecular structure for this state. The scattering length and the effective range were determined from the two lowest energy levels in [5, 6] and, using the effective range formula, bound states were found at about 40 MeV below the respective KD and KD^* thresholds. These were identified with the scalar $D_{s0}^*(2317)$ and axial $D_{s1}^*(2460)$ states respectively.

Actually, the two lower levels employed in the analysis of [5, 6] are separated by 130 MeV, which makes the use of the effective range formula a bit extreme, and the information of the upper level was disregarded. In the present work we perform a reanalysis of these lattice spectra which does not rely upon the effective range formula and takes advantage of the information of the three levels. The analysis is done using the auxiliary potential method [7], equivalent to the one of Lüscher [8, 9] in single or coupled channels, but allowing also to obtain phase-shifts for arbitrary energies. The lattice simulations are particularly suited for this kind of study because, for the same value of L , they produce

several energy levels which provide information on the energy dependence of the potential needed to interpret the spectra.

We first perform a single channel analysis, with KD or KD^* , which permits determining the two parameters of an energy dependent potential from a fit to the three energy levels of the box. This potential is then used in the continuum, leading to poles of the KD and KD^* scattering amplitudes, which lie about 40 MeV below the respective thresholds. A reformulation of the Weinberg compositeness condition [10, 11] is then used to determine the amount of KD and KD^* in the respective wave functions. A different method to learn about the amount of meson component, or equivalently the amount of non-meson component, Z , in the wave function, is from the dependence of the spectrum on the twisting angle, imposing twisted boundary conditions on the fermion fields [12].

The compositeness condition was extended leading to a new sum rule in an arbitrary number of coupled channels [13], which is reformulated in [14–18] for the case of energy dependent potentials. The sum rule contains two terms (see eq. (133) in [17]), one involving the derivative of the two-particle loop function, which is identified with the probability of the state containing this particular two-particle component of the coupled channels. The second term involves the derivative of the potential with respect to the energy, which accounts for the probability of the state to be in other components not explicitly considered in the approach, for example omitted two-meson channels or $\bar{q}q$. An illustrative example is given in [19], where one starts from a two channel problem with energy independent potentials which generate dynamically a bound state. The problem is then reformulated in terms of one channel and an effective potential, which however becomes energy dependent. This allows one to see that the term in the sum rule involving the derivative of the loop function accounts for the probability of the channel retained, while the term involving the derivative of the potential accounts for the probability of the omitted channel.

Having this in mind, we repeat the analysis of the lattice results using a two channel basis, involving $KD, \eta D_s$ for $D_{s0}^*(2317)$ and $KD^*, \eta D_s^*$ for $D_{s1}^*(2460)$. The choice of channels relies on the results of coupled channels unitary approaches [20–29], which found those channels to be the relevant ones (in what follows we will mainly refer to refs. [22, 23] when we give details of the coupled-channel formulation). Alternative scenarios for a non $\bar{q}q$ structure of these states have been also given [30–35]. With two channels and three energy levels one is forced to treat the three components of the coupled-channel potential (V_{11}, V_{12}, V_{22}) as being energy independent. We observe that a fit to the energy levels is not possible in this case, indicating that these levels carry no information on the ηD_s and ηD_s^* channels. This can be explained since no interpolators of this type were used in [5], while it was also found there that the levels obtained were tied to the interpolators used. Further lattice information will be needed in the future to make progress in this direction and learn more about the components that build up the $D_{s0}^*(2317)$ and $D_{s1}^*(2460)$ wav functions.

With the available limited lattice information, we can confirm that the bound states of KD and KD^* can be associated to the $D_{s0}^*(2317)$ and $D_{s1}^*(2460)$ states. We also confirm that these bound states are mostly of KD or KD^* nature, estimating about 70 % the probability of these components in their respective wave function.

The compositeness of the $D_{s0}^*(2317)$ based on indirect lattice data was first discussed in [26], but employing a different method. The scattering lengths of other scattering channels, free from disconnected diagrams, were obtained on the lattice and used to determine the parameters of their effective field theory, which was subsequently used to indirectly determine the scattering parameters of KD scattering and the pole position in this channel. Similarly, the scattering lengths from the simulation of ref. [26] were employed in [28, 29] to fix the low-energy constants of a covariant chiral unitary theory, which was then used to also identify, as composite states, the heavy-quark spin and flavour symmetry counterparts of the D_{s0}^* .

As mentioned above, additional lattice information could help us improve our knowledge on the additional building blocks that these states might have. Indeed, preliminary spectra for these channels obtained including KD , $\bar{s}c$ as well as ηD_s interpolating fields have been presented in [36]. Their plan is to perform a two-coupled channel analysis using a parametrization of the scattering matrix on the energy. This strategy has recently lead to the first results of the two-coupled channel system $K\pi - K\eta$ from lattice QCD; the pole positions of the scattering matrix were subsequently found and related to the strange mesons [37]. The approach presented here offers an alternative way to extract physical information from the lattice spectra in the future.

2 Compositeness of states

We collect here the essential expressions relevant to interpret the nature of hadrons generated dynamically from a given meson-meson interaction. Let us take two mesons (K and D for example) and an interacting potential V . The Lippmann-Schwinger equation produces the scattering amplitude T

$$T = V + VGT, \tag{2.1}$$

where G stands for the two meson propagator. We shall take relativistic propagators and eq. (2.1) will be the Bethe-Salpeter equation. The on-shell factorization of V and T allows one to convert eq. (2.1) into an algebraic equation with G given by

$$G = i \int \frac{d^4q}{(2\pi)^4} \frac{1}{q^2 - m_1^2 + i\epsilon} \frac{1}{(P - q)^2 - m_2^2 + i\epsilon}, \tag{2.2}$$

where P is the total two meson momentum. This factorization was justified in refs. [38, 39] by using dispersion relations in which the smooth energy dependent contribution of the left-hand-side cut was replaced by a constant in the region of interest. The energy dependence was shown to be particularly weak in the case of the meson-baryon interaction [39] due to the large baryon mass and, consequently, it will be even weaker in the present case due to the larger mass of the D and D^* mesons. The neglect of the left hand cut is also inherent in the Lüscher formalism, as we shall see in section 3.2.

Upon integration of the q^0 variable the loop function becomes

$$G = \int \frac{d^3q}{(2\pi)^3} I(\vec{q}), \quad I(\vec{q}) = \frac{\omega_1(\vec{q}) + \omega_2(\vec{q})}{2\omega_1(\vec{q})\omega_2(\vec{q}) [P^2 - (\omega_1(\vec{q}) + \omega_2(\vec{q}))^2 + i\epsilon]}, \tag{2.3}$$

where $\omega_i(\vec{q})$ is the meson on-shell energy. The loop function must be conveniently regularized with a cut-off q_{\max} , or employing dimensional regularization techniques.

Assume now the Bethe-Salpeter equation projected over S -wave and V an energy independent potential in one channel (say KD). We then have

$$T(1 - VG) = V, \quad T = \frac{V}{1 - VG} = \frac{1}{V^{-1} - G}. \quad (2.4)$$

Let us now assume that the interaction V produces a bound state, which we will refer to as a two meson composite state or a dynamically generated state. We shall see that the energy independent potential can not lead to a genuine state, for example a $\bar{q}q$ state with a weak coupling to two mesons. In the case of one channel, the coupling g of the bound state is obtained by requiring that around the pole $s = s_0$ (with $s = P^2$ being a Mandelstam variable)

$$T \sim \frac{g^2}{s - s_0}, \quad \text{hence : } g^2 = \lim_{s \rightarrow s_0} (s - s_0)T. \quad (2.5)$$

Since $V^{-1} - G = 0$ at the bound state pole, we find in the case of an energy independent potential using L'Hopital's rule

$$g^2 = \frac{1}{-\frac{\partial G}{\partial s}}, \quad -g^2 \frac{\partial G}{\partial s} = 1. \quad (2.6)$$

The property of eq. (2.6) can be generalized to coupled channels and, in the case of an energy independent potential (and two channels), one finds:

$$V = \begin{pmatrix} V_{11} & V_{12} \\ V_{12} & V_{22} \end{pmatrix}, \quad G = \begin{pmatrix} G_1 & 0 \\ 0 & G_2 \end{pmatrix}, \quad (2.7)$$

$$T = (1 - VG)^{-1}V, \quad (2.8)$$

$$g_i g_j = \lim_{s \rightarrow s_0} (s - s_0) T_{ij}, \quad \sum_i \left(-g_i^2 \frac{\partial G_i}{\partial s} \right) = 1 \quad (2.9)$$

Equation (2.6) is a reformulation of the Weinberg compositeness condition [10], which is usually applied to loosely bound states, meant to be used at higher binding energies, while eq. (2.9) is the extension to many coupled channels [13]. By solving the Schrödinger equation in momentum space in coupled channels and normalizing the wave function of the bound state to unity, it was found [13]

$$\int d^3p |\langle p | \Psi_i \rangle|^2 = g_i^2 \frac{\partial G_i}{\partial E}, \quad (2.10)$$

with $|\Psi_i\rangle$ being the i component of the bound state in the i^{th} channel, so that each term of the sum in eq. (2.9) represents the probability to have this channel in the wave function of the bound state:¹

$$P_i = -g_i^2 \frac{\partial G_i}{\partial s}, \quad (2.11)$$

¹As discussed in [13] there is a different normalization of the amplitudes, and hence the couplings, between [13] and field theoretical approach used here, which leaves the probability to be expressed here as in eq. (2.11)

and the sum of these probabilities saturates the wave function. Note that, by construction, in the case we are discussing here all the components of the composite state are of meson-meson type. We will elaborate more on these issues in section 5.

It is easy to visualize a genuine state that couples weakly to a meson-meson component by using a meson-meson potential of the type:

$$V = \frac{b}{s - s_R}, \tag{2.12}$$

which we refer to as a CDD pole [41]. Now

$$T = \frac{1}{\frac{s - s_R}{b} - G}, \quad g^2 = \frac{1}{\frac{1}{b} - \frac{\partial G}{\partial s}}, \tag{2.13}$$

and

$$P = -g^2 \frac{\partial G}{\partial s} = 1 - g^2 \frac{1}{b}. \tag{2.14}$$

In the limit of $b \rightarrow 0$ (small coupling of the genuine state to meson-meson) we have $g^2 \rightarrow 0$ and the pole appears at $s = s_R$. Then the amount of meson-meson component, $-g^2 \partial G / \partial s$, goes to zero and we have a representation for a genuine state, or, in general, a state different from the explicit two meson state considered. It is interesting to note a distinct feature in the potential of eq. (2.12), namely its energy dependence.

These ideas are generalized in ref. [17], with the sum rule

$$-\sum_i g_i^2 \frac{\partial G_i}{\partial s} - \sum_{i,j} g_i g_j G_i \frac{\partial V_{i,j}}{\partial s} G_j = 1, \tag{2.15}$$

evaluated at the pole. The first term in eq. (2.15) is associated in ref. [17] to the composite part of the state (meson-meson in the present case) and the second term, involving the derivative of the potential, to the genuine part of the state. Actually, this second part accounts for the state components that have not been considered in the coupled channel problem. This is easily shown in the case of two channels in ref. [19], where one channel is eliminated and its effects are accounted for by means of an effective potential in the remaining channel. Take $V_{22} = 0$, for simplicity, and consider V_{ij} energy independent to saturate the state with the two channels in eq. (2.7). It is then easy to obtain from eq. (2.8),

$$T_{11} = \frac{V_{11} + V_{12}^2 G_2}{1 - (V_{11} + V_{12}^2 G_2) G_1}, \tag{2.16}$$

making clear that solving a one-channel problem with the effective potential

$$V_{\text{eff}} = V_{11} + V_{12}^2 G_2, \tag{2.17}$$

gives the same amplitude T_{11} obtained in the two channel case. The novelty is that now V_{eff} becomes energy dependent. Then, the term $-g_1^2 \partial G_1 / \partial s$, which accounts for the probability of channel 1 in the state, is the same in both formulations and the second term in eq. (2.15) is, by construction of V_{eff} , the probability of the second channel that has been eliminated. We are going to use these findings to analyze the lattice spectra of ref. [5].

	KD channel	KD^* channel
E_1 (MeV)	2086 (34)	2232 (33)
E_2 (MeV)	2218 (33)	2349 (34)
E_3 (MeV)	2419 (36)	2528 (53)

Table 1. Energy levels for the scalar (KD) and axial (KD^*) channels found in the simulation ref. [5]. The relative errors in the lattice spacing a and in aE have been added in quadrature. Only the energy differences, for example $E_n^{\text{lat}} - \bar{m}_{D_s}^{\text{lat}}$ with $\bar{m}_{D_s}^{\text{lat}} = \frac{1}{4}(m_{D_s} + 4m_{D_s^*}) = 1.8407(6)$ MeV, can be compared to the experiment.

3 Analysis of the lattice spectra

The lattice simulation of ref. [5] obtained three energy levels in the scalar channel using the KD and $\bar{s}c$ interpolators, and three² levels in the axial channel using the KD^* and $\bar{s}c$ interpolators. Table 1 collects the levels of ensemble (2),³ with $N_f = 2 + 1$ and close-to-physical pion mass $m_\pi = 156$ MeV. The lattice spacing is $a = 0.0907(13)$ fm and the box size $L = 2.90$ fm. The kaon with mass $m_K = 504(1)$ MeV obeys the usual relativistic dispersion relation $E_K(p) = (m_K^2 + p^2)^{1/2}$.

The simulation [5, 6] treated the charm quark using the so-called Fermilab method, where the leading discretization errors related to the charm quark cancel in the energy differences (with respect to the reference mass of a meson containing the same number of charm quarks). We employ the dispersion $E(p)$ for D and D^* mesons determined in the simulation of ref. [5]

$$E_{D(D^*)}(\vec{p}) = M_1 + \frac{\vec{p}^2}{2M_2} - \frac{(\vec{p}^2)^2}{8M_4^3}, \quad m_{D(D^*)} = M_1 \quad (3.1)$$

where M_1, M_2, M_4 are given in table 2.

3.1 Analysis by means of the effective range formula

In ref. [5] the scattering length and effective range for KD and KD^* scattering were obtained using only the two lowest energy levels of the lattice simulation and employing Lüscher's approach to extract the infinite volume phase shifts. In this section we analyze these results by means of an effective range formula to obtain the binding energy of the state and check the fulfillment of the sum-rule of eq. (2.6).

²The second level in the axial channel of ref. [5] is attributed to the $D_{s1}(2536)$ resonance in KD^* d-wave scattering and is therefore not used in the present paper which considers KD^* scattering in s-wave. In principle $L = 0$ and $L = 2$ can mix for $J = 1$, but using arguments of Heavy Quark Spin Symmetry [40], the spin of the heavy quark \vec{S}_Q is conserved, and so is \vec{J} , and hence $\vec{J} - \vec{S}_Q$, which can be constructed from \vec{L} and the spin 1/2 of the light quark of the D^* . For $L = 0$, $\vec{J} - \vec{S}_Q$ only has modulus 1/2, and for $L = 2$, it can have the values 3/2 and 5/2. Thus, $L = 0$ and $L = 2$ do not mix at leading order in the $O(1/m_Q)$ expansion.

³Results of set 2 in [5] are used in the axial channel.

	D meson	D^* meson
M_1 (MeV)	1639	1788
M_2 (MeV)	1801	1969
M_4 (MeV)	1936	2132

Table 2. M_i from the dispersion relation $E(p)$ (3.1) for D and D^* mesons. The rest energies, i.e. the masses M_1 , can be compared to experiment via the difference $M_1^{\text{lat}} - \bar{m}_D^{\text{lat}}$ with $\bar{m}_D^{\text{lat}} = \frac{1}{4}(m_D + 4m_{D^*}) = 1.751(3)$ MeV [5].

Channel	a_0 [fm]	r_0 [fm]	B [MeV]	$ g $ [GeV]	$-g^2 \partial G / \partial s$
KD	-1.33(20)	0.27(17)	38(9)	12.6(1.5)	1.14(0.15)
KD^*	-1.11(0.11)	0.10(0.10)	44(6)	12.6(0.7)	0.96(0.06)

Table 3. Binding energy B , meson-meson coupling $|g|$ and sum-rule [eq. (2.6)], for the bound states obtained in the lattice QCD simulation of ref. [5], analyzed using an effective range formula.

The effective range approximation reads

$$p \cot \delta = \frac{1}{a_0} + \frac{1}{2} r_0 p^2, \quad T = -\frac{8\pi E}{p \cot \delta - ip}. \quad (3.2)$$

Below threshold, one writes $p = i\tilde{p}$, and a pole of the T matrix is obtained for $\cot \delta = i$. Therefore, the pole appears for the value of \tilde{p} that satisfies

$$\frac{1}{2} r_0 \tilde{p}^2 - \tilde{p} - \frac{1}{a_0} = 0. \quad (3.3)$$

Taking random a_0 and r_0 values within the range determined by the lattice simulation [5], quoted in table 3, we obtain a series of values for the bound momentum \tilde{p} and the corresponding binding energy

$$B = -\frac{\tilde{p}^2}{2\mu}, \quad \mu = \frac{m_K m_{D/D^*}}{m_K + m_{D/D^*}}. \quad (3.4)$$

The average value of the binding energy for the KD state, which is associated to the $D_{s0}^*(2317)$, is then found to be 38(9) MeV. We note that the unitary coupled-channel approach of [22] generates such a state from the interaction of the KD and ηD_s channels mostly. Had we used the central values of a_0 and r_0 directly, we would have obtained $B = 35.8$ MeV, which obviously lies within the error bar of the results quoted in table 3. We note that this value is 0.8 MeV smaller than the one given in [5], essentially because in the present analysis we have used the (isospin averaged) physical masses of the mesons instead of the lattice ones. Employing the same procedure, we find a KD^* state with a binding energy of 44(6) MeV, which we associate to the $D_{s1}^*(2460)$. In the unitary coupled-channel approach this state is mainly built from KD^* and ηD_s^* components [23].

It is interesting to test the sum rule of eq. (2.6) for the states obtained. The g^2 at the pole can be expressed as

$$g^2 = \frac{16\pi s \tilde{p}}{\mu(1 - r_0 \tilde{p})}, \quad (3.5)$$

and listed in table 3. Since $\partial G/\partial s$ is convergent, we obtain the sum rules quoted in the last column, which, within errors, are all compatible with unity. The coupling to the KD channel is $g_{KD} = 12.6 \text{ GeV}$, which is of the order of the one obtained in the chiral unitary approach in ref. [22], $g_{KD} = 10.21 \text{ GeV}$. Note, however, that this smaller value would provide a probability for the KD channel of about 60 – 70%, leaving room for the other channels considered in the unitary coupled-channel approach. Similarly, in the KD^* channel, we find a coupling $g_{KD^*} = 12.6 \text{ GeV}$, compared to the value of around 10 GeV quoted in ref. [23], also leaving room for the additional meson-meson components considered in that work.

Although the results obtained with the effective range formula are qualitatively reasonable, and the existence of the bound state emerges as a solid statement, one can see that the approximation has its limitations when one looks at other magnitudes like the probability $P(KD)$, which comes out larger than one (although compatible within errors). There is also the fact that the first two levels are separated by 132 MeV, which makes this approximation a bit extreme. Furthermore, the information of the third level is not used, and, as shown in ref. [5], this level cannot be accounted for by means of the effective range formula. All these reasons advise a new reanalysis which we offer in the next subsection.

3.2 Analysis of lattice spectra by means of an auxiliary potential

First, we are going to make the analysis with only one channel. Anticipating that the ηD_s and ηD_s^* channels also play a role in the $D_{s0}^*(2317)$ and $D_{s1}(2460)$ resonances, as found in refs. [22] and [23], we shall leave room for these and possible $\bar{q}q$ components, by using an energy dependent potential. As a first step we take a potential linear in s ,

$$V = \alpha + \beta(s - s_{\text{th}}), \tag{3.6}$$

with $s_{\text{th}} = (M_{D^{(*)}} + M_K)^2$, since only the derivative of the potential is needed to obtain the sum rule. Later on we shall also use another type of potential.

In the finite box, the T matrix of eqs. (2.1) and (2.4) is replaced by

$$\tilde{T} = \frac{1}{V^{-1} - \tilde{G}}, \tag{3.7}$$

where \tilde{G} is the two meson loop function in the box given by [42]

$$\tilde{G} = G + \lim_{q_{\text{max}} \rightarrow \infty} \left[\frac{1}{L^3} \sum_{q_i}^{q_{\text{max}}} I(\vec{q}_i) - \int_{q < q_{\text{max}}} \frac{d^3q}{(2\pi)^3} I(\vec{q}) \right]; \quad \vec{q}_i = \frac{2\pi}{L} \vec{n}_i, \quad \vec{n}_i \in \mathbb{Z}^3. \tag{3.8}$$

The G in the continuum, eq. (2.3), can be regularized with a cut-off q'_{max} or employing dimensional regularization. The latter choice, followed in ref. [42], cannot be applied here because we employ the dispersion relation of eq. (3.1). For this reason we adopt the cut-off method, with a cut-off value that gives equivalent results to those of the chiral unitary approach of refs. [22, 23]. Any value of q'_{max} can, in principle, be taken since changes in G can be accommodated by changes in V^{-1} when we require that \tilde{T} has poles at the energies of the lattice spectra by demanding that $V^{-1} - \tilde{G} = 0$. Note, in addition, that we are

interested finally in results for the continuum. Hence, at the energies of the lattice spectra we have $V^{-1} = \tilde{G}$, and then the continuum T matrix is

$$T = \frac{1}{V^{-1} - G} = \frac{1}{\tilde{G} - G} = \frac{1}{\lim_{q_{\max} \rightarrow \infty} \left[\frac{1}{L^3} \sum_{q_i}^{q_{\max}} I(\vec{q}_i) - \int_{q < q_{\max}} \frac{d^3 q}{(2\pi)^3} I(\vec{q}) \right]}, \quad (3.9)$$

which is then independent of the cut-off q'_{\max} employed to regularize G . However, in the transfer of strength from G to V^{-1} one will be introducing some energy dependence in V^{-1} that would change the probability Z of not having the main meson-meson component considered. We shall come back to this issue in section 5 where systematic uncertainties are studied.

Equation (3.9) is the formulation employed in the approach of ref. [7], where it is shown that Lüscher formula is recovered if some terms of $I(\vec{q})$, which are exponentially suppressed, are eliminated. These terms can be relevant in the case of relativistic particles and small volumes [43, 44], which is not the case here. However, we cannot use the standard Lüscher approach either, based on the relativistic relationship $\omega(q) = (m^2 + q^2)^{1/2}$, since we are forced to employ the dispersion relation of eq. (3.1). In this case, eq. (3.9) gives the appropriate extension of the Lüscher formalism.

There is another approximation inherent in our approach (or the one of Lüscher) when we assume that the potential is volume independent. Within the framework of the chiral unitary approach such effects were investigated in [45, 46] in the $\pi\pi$ scattering in the scalar sector and the ρ sector and it was concluded that for values of $Lm_\pi > 1.5$ they could be safely neglected. In the present case, given the large masses involved, loops in the t-channel, which originate this volume dependence, are even less relevant.

With the formalism exposed above, a best fit is carried to the three lattice levels obtained in [5], demanding that the \tilde{T} derived from eq. (3.7) using the potential of eq. (3.6) has poles at the three energies. In order to find the desired magnitudes and associated statistical errors, we perform a series of fits to different sets of three energies, generated with a Gaussian weight within the errors of the lattice levels. With the parameters obtained in each fit we evaluate the different magnitudes. From the results obtained in the different fits, we then determine the central values and statistical errors of these magnitudes.

We show in figures 1 and 2 the results obtained from the fits to the levels for the KD and KD^* systems, respectively. The procedure outlined above gives us a pole for the KD system with binding energy

$$B(KD) = m_D + m_K - E_B(KD) = 46 \pm 21 \text{ MeV}, \quad (3.10)$$

to be compared to the value 36.6(16.6)(0.5) MeV obtained with the effective range formula in [5, 6] and to the 45 MeV binding in the physical case. For the KD^* system we get the binding energy

$$B(KD^*) = m_{D^*} + m_K - E_B(KD^*) = 52 \pm 22 \text{ MeV}. \quad (3.11)$$

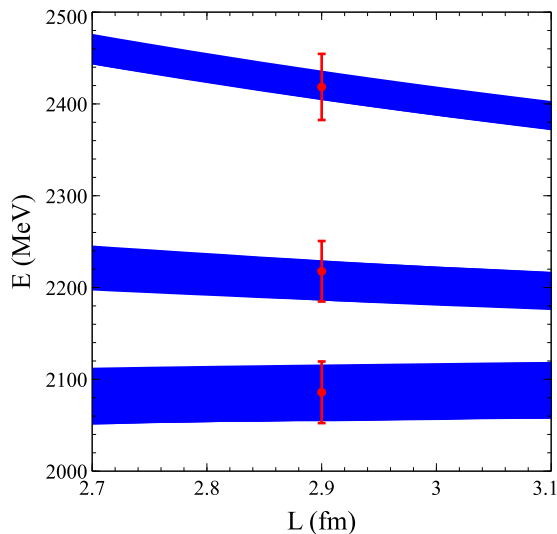


Figure 1. Fits to the lattice data of ref. [5] for the KD system using the potential of eq. (3.6).

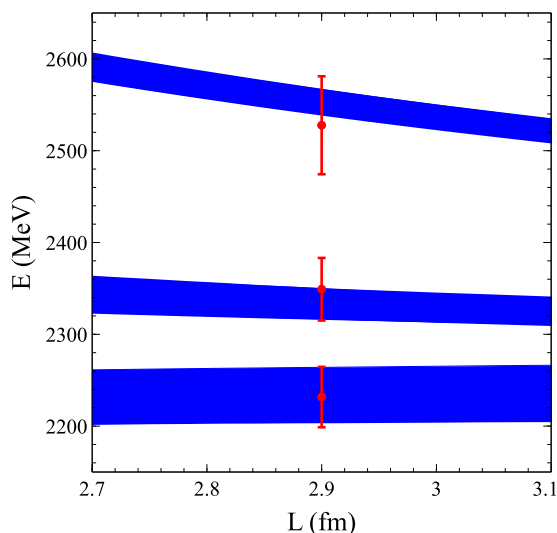


Figure 2. Fits to the lattice data of ref. [5] for the KD^* system using the potential of eq. (3.6).

The probabilities for the KD , KD^* components, obtained from eqs. (2.11), (2.5), are:

$$P(KD) = (76 \pm 12) \%, \text{ for the } D_{s0}^*(2317), \quad (3.12)$$

$$P(KD^*) = (53 \pm 17) \%, \text{ for the } D_{s1}(2460). \quad (3.13)$$

This means that there is a large amount of KD and KD^* components in the corresponding bound states.

3.3 Fit with a CDD pole

One near-threshold level was found in [5, 6] when only $\bar{s}c$ interpolators were used,⁴ and one wonders what is the $\bar{s}c$ component in the meson states at hand. We therefore explore

⁴Its energy however changes when $D^{(*)}K$ interpolators were used in addition to $\bar{s}c$ ones.

whether there could be an admixture of some genuine component in the bound state by refitting the lattice levels adding a CDD pole to the potential of eq. (3.6):

$$V = \alpha + \beta(s - s_{\text{th}}) + \frac{\gamma^2}{s - M_{\text{CDD}}^2}, \quad (3.14)$$

which, as seen in section 2, is suited to accommodate a genuine state. This has been shown to be the proper way to account for genuine components in different works [19, 38, 47, 48] in the continuum. An analysis of “synthetic” lattice spectra in terms of this potential was done in [42]. It was also recently employed to analyze lattice spectra with the πK and ηK channels in [37].

Since we have four parameters (α , β , γ and M_{CDD}) and three energy levels, we can obtain solutions with many sets of parameters which are, obviously, correlated. However, the values of the parameters do not have a particular significance and what matters is the value of the magnitudes derived from the different fits. The statistics of the obtained fits shows a clear preference for solutions with a M_{CDD} value that lies far away (more than 300 MeV) from the KD , KD^* thresholds, such that it effectively provides a linear dependence in $(s - s_{\text{th}})$ at the energies where the poles are found. This is an indication that the lattice energies do not favour a CDD component, or at least not a significant one. Obviously, future lattice results with more accuracy and different volumes will allow one to be more precise on this issue.

With the potential of eq. (3.14) we obtain the following binding energies

$$B(KD) = 29 \pm 15 \text{ MeV}, \quad (3.15)$$

$$B(KD^*) = 37 \pm 23 \text{ MeV}, \quad (3.16)$$

and probabilities

$$P(KD) = (67 \pm 14) \%, \text{ for the } D_{s0}^*(2317), \quad (3.17)$$

$$P(KD^*) = (61 \pm 26) \%, \text{ for the } D_{s1}(2460), \quad (3.18)$$

which are compatible within errors with those of eqs. (3.10)–(3.13), obtained with the linear potential.

3.4 Two channel analysis

After this exercise we perform a two channel analysis including the ηD_s channel for the $D_{s0}^*(2317)$ state and the ηD_s^* channel for the $D_{s1}(2460)$, which were found also relevant in refs. [22, 23].

Since we only have three energy levels we use an energy independent potential, eq. (2.7), which has three parameters, V_{11} , V_{12} , V_{22} . By doing so, we would force the states to saturate with the $KD^{(*)}$, $\eta D_s^{(*)}$ components. The comparison of the two procedures would allow us to make statements about the amount of each channel in the respective states.

We thus fit the V_{ij} parameters using

$$\tilde{T} = (1 - V\tilde{G})^{-1}V, \quad (3.19)$$

in two channels, looking for the poles of \tilde{T} and associating the first three levels to those of the lattice simulation.

We do not find any suitable fit to the data, which is an enlightening result. One could interpret it as an evidence that the energy levels obtained in [5] do not contain information on the ηD_s or ηD_s^* channels. This seems to be the case because the three energies obtained there were tied to the use of $q\bar{q}$ and meson-meson interpolators of KD or KD^* type. No interpolator was used containing information on the ηD_s and ηD_s^* channels, and no energy level was found which would be tied to these channels. It is indeed a common experience of lattice practitioners that a given two-hadron eigenstate is most often not seen unless explicitly implemented in the basis of interpolating fields. Although all states with a given quantum number are in principle expected in a dynamical simulation, a poor basis of interpolating fields is insufficient to render them in practice. The reason is that one would have to wait much time till these components show up in the time evolution of the state and this could happen in the region where the ratio of noise to signal is large, preventing any signal to be seen [49]. This also gives us some idea on how to proceed in the future if one wishes to make progress on determining the components of the $D_{s0}^*(2317)$ and $D_{s1}(2460)$ wave functions. The relevant fraction of the wave function that went to the ηD_s and ηD_s^* channels in chiral unitary studies [22, 23], of the order of 20%, makes it advisable to include interpolators for the ηD_s and ηD_s^* channels in future lattice simulations. Such a simulation is underway and preliminary spectra have been presented in [36]. . In any case, it is worth stressing that, as shown in previous sections, the present lattice information allows to conclude that there are extra components to the dominant KD in the $D_{s0}^*(2317)$ wave function, although one cannot state which ones.

4 Scattering length and effective range

We can also obtain the scattering length and the effective range in each of the cases explored. For this we use eq. (3.2), finding

$$p \cot \delta = \text{Re} \left\{ -\frac{8\pi E}{T} \right\} \simeq \frac{1}{a_0} + \frac{1}{2} r_0 p^2 . \quad (4.1)$$

Relating E to p via the dispersion relation of eq. (3.1)

$$E = \sqrt{m_K^2 + p^2} + E_{D(D^*)}(p) , \quad (4.2)$$

we obtain

$$a_0 = -1.2 \pm 0.6 \text{ fm}, \quad r_0 = 0.04 \pm 0.16 \text{ fm for } KD, \quad (4.3)$$

$$a_0 = -0.9 \pm 0.3 \text{ fm}, \quad r_0 = -0.3 \pm 0.4 \text{ fm for } KD^* \quad (4.4)$$

in the case the lattice data is analyzed using a single channel potential (3.6).

When we use the CDD potential of eq. (3.14) we find

$$a_0 = -1.4 \pm 0.4 \text{ fm}, \quad r_0 = -0.2 \pm 0.4 \text{ fm for } KD, \quad (4.5)$$

$$a_0 = -1.3 \pm 0.6 \text{ fm}, \quad r_0 = -0.1 \pm 0.2 \text{ fm for } KD^* \quad (4.6)$$

The values for the scattering length and effective range obtained with the different methods are remarkably similar.

The values obtained also agree qualitatively with those obtained in ref. [5]. Yet, as we have discussed, we do not use the effective range formula to correlate the results. Indeed, instead of eq. (4.1) we have

$$p \cot \delta = -8\pi E(V^{-1} - \text{Re}\{G\}) \tag{4.7}$$

and the G function depends on the cut off. If V is energy independent we have two degrees of freedom in the approach to accommodate the values of a_0 and r_0 , but $p \cot \delta$ develops terms in p^4 which are tied to the values of a_0 and r_0 . If we allow V to be energy dependent, as in eq. (3.6), we have more freedom to accommodate the p^4 terms in the expansion of $p \cot \delta$. However, the main problem in the use of eq. (4.1) is that it blows up at large energies, where the series expansion does not converge. Our method, which does not make a series expansion of $p \cot \delta$, has a good behavior at higher energies from the analytical behavior of $\text{Re}\{G\}$, which contains the *log* terms of the intermediate particle propagators. This allows us to cover a wider span of energies and we can make use of the three energy levels obtained in [5], while only the information of the lowest two could be accommodated in the analysis of [5] based on eq. (4.1).

5 Evaluation of systematic uncertainties

In [26] the lowest lattice level obtained for the channels $D\bar{K}(I = 1)$, $D\bar{K}(I = 0)$, $D_s K$, $D\pi(I = 3/2)$, $D_s \pi$, free from disconnected diagrams, were employed to obtain, via the Lüscher formalism [10], the phase shifts in the continuum at the eigenenergies of the lattice box. The scattering length was then derived from the relationship $p \cot \delta(p) = 1/a_0$, disregarding the effective range term. The low energy constants of a chiral lagrangian were fitted to the scattering lengths of those channels employing a unitary approach. With these values of the coefficients, the coupled KD , ηD_s channels system was studied, from where the existence of a bound state associated to the $D_{s0}^*(2317)$ was established and the KD scattering length was obtained. A KD probability, $1 - Z$, in the $D_{s0}^*(2317)$ wave function of around 70% was found, where the value of Z was determined from the scattering length via the relation [10, 11]

$$a_0 = -2 \frac{(1 - Z)}{(2 - Z)} \frac{1}{\sqrt{2\mu\epsilon}} \left[1 + \mathcal{O}(\sqrt{2\mu\epsilon}/\beta) \right], \tag{5.1}$$

with μ and ϵ being the reduced mass and binding energy, respectively, and $1/\beta$ accounting basically for the range of the interaction ($1/q_{\text{max}}$ in our approach). The term $\mathcal{O}(\sqrt{2\mu\epsilon}/\beta)$, negligible for small binding energies, is often discussed as uncertainty. In the present case $\sqrt{2\mu\epsilon}/\beta$ is of the order of 0.22 if we take $\beta = q_{\text{max}} = M_V = 780$ MeV, and the correcting terms can be relevant.

Indeed, let us comment on the sensitivity of eq. (5.1) in obtaining Z from the value of a_0 . Note that if $-2/\sqrt{2\mu\epsilon} < a_0 < -1/\sqrt{2\mu\epsilon}$, the resulting Z would have unphysical negative values. This condition would obviously not be a problem for sufficiently small binding

energies where eq. (5.1) is applicable but, for the KD state analyzed here, the value of the factor $-1/\sqrt{2\mu\epsilon}$ is -1.12 fm, close to the typical values found for the scattering lengths, and this can lead to large uncertainties in the extraction of Z from a_0 using eq. (5.1). Note that ref. [26] obtained $a_0 \sim -0.85$ fm, from which, using eq. (5.1), a probability $P_{KD} \sim 70\%$ was extracted, similar to the result obtained here in spite of the fact that we have a different value of the scattering length.

Incidentally, one could have evaluated $P = 1 - Z$ directly from the coupling also in the Weinberg approach using eq. (24) from ref. [10], which is equivalent to eq. (2.11) used here but neglecting the $\mathcal{O}(\sqrt{2\mu\epsilon}/q_{\max})$ terms in $(\partial G/\partial s)$ and in the determination of g_i^2 . It is instructive to see the correcting terms in $(\partial G/\partial s)$ due to the range of the interaction. Using, for simplicity, the nonrelativistic approach of [13] (see eqs. (27), (29) there) one finds

$$\frac{\partial G}{\partial E} = \frac{1}{\gamma} 8\pi\mu^2 \left[\arctan\left(\frac{q_{\max}}{\gamma}\right) - \frac{\gamma q_{\max}}{\gamma^2 + q_{\max}^2} \right] \tag{5.2}$$

$$= \frac{1}{\gamma} 8\pi\mu^2 \left[\frac{\pi}{2} - 2\left(\frac{\gamma}{q_{\max}}\right) + \frac{4}{3}\left(\frac{\gamma}{q_{\max}}\right)^3 + \dots \right] \tag{5.3}$$

$$= \frac{1}{\gamma} 4\pi^2\mu^2 \left[1 - \frac{4}{\pi}\left(\frac{\gamma}{q_{\max}}\right) + \frac{8}{3\pi}\left(\frac{\gamma}{q_{\max}}\right)^3 + \dots \right]. \tag{5.4}$$

Hence, in the nonrelativistic expression

$$1 - Z = g^2 \frac{\partial G}{\partial E}, \tag{5.5}$$

analogous to eq. (2.11), the correcting factor to the Weinberg formula from range effects in $\partial G/\partial E$ is:⁵

$$F = \left[1 - \frac{4}{\pi}\left(\frac{\gamma}{q_{\max}}\right) + \frac{8}{3\pi}\left(\frac{\gamma}{q_{\max}}\right)^3 + \dots \right]. \tag{5.6}$$

to which one would have to add the correcting terms to the expression of g^2 in ref. [10]. The deviation from unity of eq. (5.6) in the problem analyzed here amounts to 28%. Although one would also have correcting terms from g^2 , this exercise gives us an idea of the order of magnitude of the corrections due to finite range effects in the determination of $1 - Z$. The exercise also serves us another purpose, which is to note that employing eq. (24) from ref. [10] can give reasonable numbers for $1 - Z$ in the present case, within uncertainties, while applying eq. (5.1) is not possible for a value $a_0 \sim -1.3$ fm. Actually, in ref. [50], following the work of [26], the value of $a_0 \sim -1.33$ fm from the lattice work of [6] is used as input to further constrain the parameters of the chiral theory, but eq. (5.1) is no longer used. In our case we do not use eq. (5.1), nor eq. (24) from ref. [10], in order to determine $1 - Z$, but eq. (2.11) in which explicit range effects will appear in g^2 and $\partial G_i/\partial s$ from our formulation of the problem using eq. (2.4) for the scattering of the particles. This is our prescription to take into account range effects and we discuss next the sensitivity of the results to the changes of the range parameter q_{\max} , also within our approach.

⁵The normalizations for g in [12] and here are different. In [12], or in the Weinberg notation, $\partial G/\partial E$ is used instead of $\partial G/\partial s$, but the range correcting factor, F , is the same.

q_{\max} (MeV)	770	875	1075	1275	Average
B (MeV)	34.2	36.6	35.5	35.5	35.5 ± 0.8
$ g $ (GeV)	10.85	10.60	10.37	10.41	10.6 ± 0.20
P (%)	86.68	82.15	84.09	87.16	85 ± 2
a_0 (fm)	-1.32	-1.24	-1.25	-1.25	-1.27 ± 0.03
r_0 (fm)	0.30	0.22	0.19	0.19	0.23 ± 0.05

Table 4. Dependence of the properties of the KD bound state on q_{\max} .

q_{\max} (MeV)	770	875	1075	1275	Average
B (MeV)	45.8	45.6	44.9	44.2	45.0 ± 0.7
$ g $ (GeV)	10.67	10.15	10.32	10.31	10.4 ± 0.2
P (%)	60.30	57.42	63.33	66.10	62 ± 3
a_0 (fm)	-1.010	-0.967	-0.980	-0.986	-0.99 ± 0.02
r_0 (fm)	0.07	-0.03	-0.04	-0.06	-0.02 ± 0.05

Table 5. Dependence of the properties of the KD^* bound state on q_{\max} .

We estimate the uncertainties inherent to the method for not too small binding energies, like in the present case, by performing fits to the lattice energies employing four different values of q_{\max} , 770 MeV, 875 MeV, 1075 MeV, 1275 MeV, and the auxiliary potential linear in s of eq. (3.6). This will inform us on the size of systematic uncertainties coming from this source. In order not to be confused by the statistical uncertainties, the fit for each value of q_{\max} will be done to the central values of the lattice energies. Our results, shown in table 4 for the KD system and in table 5 for the KD^* one, confirm that the systematic uncertainties tied to the range are small and well within the statistical uncertainties. The binding energy of the KD^* system shows a stronger sensitivity to the heavy meson mass employed than that of all other magnitudes, the changes of which fall well within the statistical errors.

We also have to face uncertainties tied to the meson masses employed in our analysis. Unlike in [26], the lattice spectrum used here is calculated with a pion mass of $m_\pi = 156$ MeV, already very close to the physical value of 140 MeV. Moreover, since in the present case, only the kaon and D , D^* masses appear in the propagators and the potential is fitted to the lattice energy levels, there is no explicit dependence on m_π in the analysis. We also assume that something similar occurs for the lattice energy levels and the changes between using 156 MeV or 140 MeV would be insignificant. This is actually the case for the chiral extrapolation of the $\bar{K}D$ and KD scattering lengths in [26]. However, the D and D^* masses of the lattice simulation are smaller than the physical ones, which is related to the Fermilab method employed (see M_1 in table 2). This is the reason why we did not quote absolute values of the energies obtained, but the binding energies with respect to the thresholds. We can attempt to do an extrapolation of the results to physical masses.

M_1 (MeV)	1631 Ref. [5]	1867 Physical
B (MeV)	35.5	31.9
$ g $ (GeV)	10.4	11.3
P (%)	87.2	88.3
a_0 (fm)	-1.25	-1.33
r_0 (fm)	0.19	0.14

Table 6. Extrapolation of the bound state properties to the physical mass of the D meson, using $q_{\max} = 1275$ MeV.

M_1 (MeV)	1788 Ref. [5]	2008 Physical
B (MeV)	44	96
$ g $ (GeV)	10.3	14.2
P (%)	66.1	60.6
a_0 (fm)	-0.99	-0.72
r_0 (fm)	-0.060	-0.002

Table 7. Extrapolation of the bound state properties to the physical mass of the D^* meson, using $q_{\max} = 1275$ MeV.

For this purpose we assume that the potential obtained can also be considered in absolute terms. Then we use this potential with the realistic masses in the loop function G and obtain the results shown in tables 6 and 7.

A third source of systematic uncertainties comes from the use of one type or another of the potentials, eqs. (3.6) or (3.14), that we have already discussed in sections 3.2 and 3.3, respectively. Comparing the values given in eqs. (3.10)–(3.13) with those of eqs. (3.15)–(3.18), we find that the systematic errors associated to the use of different potentials are:

$$\begin{aligned}
 \delta B(KD) &= 8.5 \text{ MeV}, \\
 \delta B(KD^*) &= 7.5 \text{ MeV}, \\
 \delta P(KD) &= 4.5 \%, \\
 \delta P(KD^*) &= 4.0 \%, \\
 \delta a(KD) &= 0.1 \text{ fm}, \\
 \delta a(KD^*) &= 0.2 \text{ fm}, \\
 \delta r_0(KD) &= 0.1 \text{ fm}, \\
 \delta r_0(KD^*) &= 0.1 \text{ fm}.
 \end{aligned}$$

Altogether, summing these systematic errors in quadrature to those of tables 4–7, we finally obtain the results:

$$\begin{aligned}
 B(KD) &= 38 \pm 18 \pm 9 \text{ MeV}, \\
 B(KD^*) &= 44 \pm 22 \pm 26 \text{ MeV}, \\
 P(KD) &= 72 \pm 13 \pm 5 \%, \\
 P(KD^*) &= 57 \pm 21 \pm 6 \%, \\
 a(KD) &= -1.3 \pm 0.5 \pm 0.1 \text{ fm}, \\
 a(KD^*) &= -1.1 \pm 0.5 \pm 0.2 \text{ fm}, \\
 r_0(KD) &= -0.1 \pm 0.3 \pm 0.1 \text{ fm}, \\
 r_0(KD^*) &= -0.2 \pm 0.3 \pm 0.1 \text{ fm},
 \end{aligned}$$

where the first error is statistical and the second systematic, which should also add in quadrature.

6 Conclusions

In this work we have done a reanalysis of the lattice spectra obtained in [5, 6] for s-wave scattering channels KD and KD^* , where bound states were identified with the $D_{s0}^*(2317)$ and $D_{s1}^*(2460)$ states. The analysis of [5, 6] derived the scattering length and the effective range from two of the energy levels. The information of the third level was not used. Here we have done a reanalysis of the lattice spectra that takes into account the information of the three levels. The essence of the new method was the use of an auxiliary potential which was allowed to be energy dependent in the case of considering only one channel. This is demanded to take into account the fact that the single channels will most probably not saturate the states. We found a bound state for both KD and KD^* scattering, which we associated to the $D_{s0}^*(2317)$ and $D_{s1}^*(2460)$ states.

In order to find out the most likely missing channels we were guided by the results of the chiral unitary approach which determines the ηD_s , and ηD_s^* channels as the additional most important ones to saturate the wave function. However, the limited information from the lattice spectra drove us to use an energy independent potential with the consequence that the two channels chosen would saturate the wave function. With this restriction we found no solution, indicating that the lattice spectra does not contain information on the ηD_s , and ηD_s^* channels. This seems to be the case since the levels found in [5] are largely tied to the interpolators used, and no interpolators accounting for ηD_s and ηD_s^* states were included.

We analyzed the lattice spectra considering only one channel and two energy dependent potentials. One potential is taken linear in s and another one contains a CDD pole accounting for possible genuine $\bar{c}s$ components. The results with both methods were compatible within errors. We also studied systematic uncertainties from other sources, which were found, in all cases but one, reasonably smaller than the statistical errors. Our analysis

confirmed the existence of bound states for the KD and KD^* channels with a binding of the order of 40 MeV, which we associated to the $D_{s0}^*(2317)$ and $D_{s1}^*(2460)$ states. We could also determine the scattering length and effective range for KD and KD^* scattering, improving on the previous results of [5] based on the information of the lowest two levels only and relying upon the effective range formula. Finally, we could determine within errors that the states found are mostly of meson-meson nature and, using a sum rule which reformulates the test of compositeness condition of Weinberg, we established the probability to find KD and KD^* in those states in an amount of about $(72 \pm 13 \pm 5) \%$ and $(57 \pm 21 \pm 6) \%$, respectively. We discussed that, in order to be more precise on these numbers and obtain information on the channels that fill the rest of the probability, one must improve on the precision of the energy spectra and must include further interpolators that allow one to include the ηD_s and ηD_s^* channels in the analysis.

The exercise done shows the power of the method and the valuable information contained in the lattice spectra. The errors obtained here can be improved by having extra accuracy in the lattice spectra, additional levels, or more easy perhaps, spectra calculated for other lattice sizes. In any case, it has become clear that the information provided by the lattice spectra, and the flexibility to use different box sizes to obtain a rich spectrum of energies, is most useful when it comes to determine the energy dependence of the auxiliary potentials, which is essential to determine probabilities of meson meson components (or hadron hadron components in general) via the generalized sum rule.

Acknowledgments

S.P. is grateful to C.B. Lang, L. Leskovec, D. Mohler and R. Woloshyn for the pleasant collaboration on the simulation that is analyzed in the present work. We would all like to thank them, and also M. Döring, for the subsequent useful discussions. A. M. T would like to thank the Brazilian funding agency FAPESP for the financial support. This work is partly supported by the Spanish Ministerio de Economía y Competitividad and European FEDER funds under contract numbers FIS2011-28853-C02-01 and FIS2011-28853-C02-02, by the Generalitat Valenciana in the program Prometeo II, 2014/068, and by Grant 2014SGR-401 from the Generalitat de Catalunya. We acknowledge the support of the European Community-Research Infrastructure Integrating Activity Study of Strongly Interacting Matter (acronym HadronPhysics3, Grant Agreement n. 283286) under the Seventh Framework Programme of EU.

Open Access. This article is distributed under the terms of the Creative Commons Attribution License ([CC-BY 4.0](https://creativecommons.org/licenses/by/4.0/)), which permits any use, distribution and reproduction in any medium, provided the original author(s) and source are credited.

References

- [1] BABAR collaboration, B. Aubert et al., *Observation of a narrow meson decaying to $D_s^+ \pi^0$ at a mass of 2.32 GeV/c²*, *Phys. Rev. Lett.* **90** (2003) 242001 [[hep-ex/0304021](https://arxiv.org/abs/hep-ex/0304021)] [[INSPIRE](https://inspirehep.net/literature/1000000)].

- [2] CLEO collaboration, D. Besson et al., *Observation of a narrow resonance of mass 2.46 GeV/c² decaying to D_s^{*+}π⁰ and confirmation of the D_{s,J}^{*}(2317) state*, *Phys. Rev. D* **68** (2003) 032002 [Erratum *ibid.* **D 75** (2007) 119908] [[hep-ex/0305100](#)] [[INSPIRE](#)].
- [3] BABAR collaboration, J.P. Lees et al., *Measurement of the mass and width of the D_{s1}(2536)⁺ meson*, *Phys. Rev. D* **83** (2011) 072003 [[arXiv:1103.2675](#)] [[INSPIRE](#)].
- [4] PARTICLE DATA GROUP collaboration, K. A. Olive et al., *Review of particle physics*, *Chin. Phys. C* **38** (2014) 090001 [[INSPIRE](#)].
- [5] C.B. Lang, L. Leskovec, D. Mohler, S. Prelovsek and R.M. Woloshyn, *D_s mesons with DK and D^{*}K scattering near threshold*, *Phys. Rev. D* **90** (2014) 034510 [[arXiv:1403.8103](#)] [[INSPIRE](#)].
- [6] D. Mohler, C.B. Lang, L. Leskovec, S. Prelovsek and R.M. Woloshyn, *D_{s0}^{*}(2317) meson and D-meson-kaon scattering from lattice QCD*, *Phys. Rev. Lett.* **111** (2013) 222001 [[arXiv:1308.3175](#)] [[INSPIRE](#)].
- [7] M. Döring, U.-G. Meißner, E. Oset and A. Rusetsky, *Unitarized chiral perturbation theory in a finite volume: scalar meson sector*, *Eur. Phys. J. A* **47** (2011) 139 [[arXiv:1107.3988](#)] [[INSPIRE](#)].
- [8] M. Lüscher, *Volume dependence of the energy spectrum in massive quantum field theories. 2. Scattering states*, *Commun. Math. Phys.* **105** (1986) 153 [[INSPIRE](#)].
- [9] M. Lüscher, *Two particle states on a torus and their relation to the scattering matrix*, *Nucl. Phys. B* **354** (1991) 531 [[INSPIRE](#)].
- [10] S. Weinberg, *Evidence that the deuteron is not an elementary particle*, *Phys. Rev.* **137** (1965) B672 [[INSPIRE](#)].
- [11] V. Baru, J. Haidenbauer, C. Hanhart, Y. Kalashnikova and A.E. Kudryavtsev, *Evidence that the a₀(980) and f₀(980) are not elementary particles*, *Phys. Lett. B* **586** (2004) 53 [[hep-ph/0308129](#)] [[INSPIRE](#)].
- [12] D. Agadjanov, F.-K. Guo, G. Ríos and A. Rusetsky, *Bound states on the lattice with partially twisted boundary conditions*, *JHEP* **01** (2015) 118 [[arXiv:1411.1859](#)] [[INSPIRE](#)].
- [13] D. Gamermann, J. Nieves, E. Oset and E. Ruiz Arriola, *Couplings in coupled channels versus wave functions: application to the X(3872) resonance*, *Phys. Rev. D* **81** (2010) 014029 [[arXiv:0911.4407](#)] [[INSPIRE](#)].
- [14] T. Hyodo, D. Jido and A. Hosaka, *Origin of the resonances in the chiral unitary approach*, *Phys. Rev. C* **78** (2008) 025203 [[arXiv:0803.2550](#)] [[INSPIRE](#)].
- [15] T. Sekihara, T. Hyodo and D. Jido, *Internal structure of resonant Lambda(1405) state in chiral dynamics*, *Phys. Rev. C* **83** (2011) 055202 [[arXiv:1012.3232](#)] [[INSPIRE](#)].
- [16] T. Hyodo, D. Jido and A. Hosaka, *Compositeness of dynamically generated states in a chiral unitary approach*, *Phys. Rev. C* **85** (2012) 015201 [[arXiv:1108.5524](#)] [[INSPIRE](#)].
- [17] T. Hyodo, *Structure and compositeness of hadron resonances*, *Int. J. Mod. Phys. A* **28** (2013) 1330045 [[arXiv:1310.1176](#)] [[INSPIRE](#)].
- [18] T. Sekihara, T. Hyodo and D. Jido, *Comprehensive analysis of the wave function of a hadronic resonance and its compositeness*, [arXiv:1411.2308](#) [[INSPIRE](#)].

- [19] F. Aceti, L.R. Dai, L.S. Geng, E. Oset and Y. Zhang, *Meson-baryon components in the states of the baryon decuplet*, *Eur. Phys. J. A* **50** (2014) 57 [[arXiv:1301.2554](#)] [[INSPIRE](#)].
- [20] E.E. Kolomeitsev and M.F.M. Lutz, *On heavy light meson resonances and chiral symmetry*, *Phys. Lett. B* **582** (2004) 39 [[hep-ph/0307133](#)] [[INSPIRE](#)].
- [21] F.-K. Guo, P.-N. Shen, H.-C. Chiang, R.-G. Ping and B.-S. Zou, *Dynamically generated 0^+ heavy mesons in a heavy chiral unitary approach*, *Phys. Lett. B* **641** (2006) 278 [[hep-ph/0603072](#)] [[INSPIRE](#)].
- [22] D. Gamermann, E. Oset, D. Strottman and M.J. Vicente Vacas, *Dynamically generated open and hidden charm meson systems*, *Phys. Rev. D* **76** (2007) 074016 [[hep-ph/0612179](#)] [[INSPIRE](#)].
- [23] D. Gamermann and E. Oset, *Axial resonances in the open and hidden charm sectors*, *Eur. Phys. J. A* **33** (2007) 119 [[arXiv:0704.2314](#)] [[INSPIRE](#)].
- [24] F.-K. Guo, C. Hanhart and U.-G. Meißner, *Interactions between heavy mesons and Goldstone bosons from chiral dynamics*, *Eur. Phys. J. A* **40** (2009) 171 [[arXiv:0901.1597](#)] [[INSPIRE](#)].
- [25] P. Wang and X.G. Wang, *Study on 0^+ states with open charm in unitarized heavy meson chiral approach*, *Phys. Rev. D* **86** (2012) 014030 [[arXiv:1204.5553](#)] [[INSPIRE](#)].
- [26] L. Liu, K. Orginos, F.-K. Guo, C. Hanhart and U.-G. Meißner, *Interactions of charmed mesons with light pseudoscalar mesons from lattice QCD and implications on the nature of the $D_{s0}^*(2317)$* , *Phys. Rev. D* **87** (2013) 014508 [[arXiv:1208.4535](#)] [[INSPIRE](#)].
- [27] M. Cleven, H.W. Griebhammer, F.-K. Guo, C. Hanhart and U.-G. Meißner, *Strong and radiative decays of the $D_{s0}^*(2317)$ and $D_{s1}(2460)$* , *Eur. Phys. J. A* **50** (2014) 149 [[arXiv:1405.2242](#)] [[INSPIRE](#)].
- [28] M. Altenbuchinger, L.S. Geng and W. Weise, *Scattering lengths of Nambu-Goldstone bosons off D mesons and dynamically generated heavy-light mesons*, *Phys. Rev. D* **89** (2014) 014026 [[arXiv:1309.4743](#)] [[INSPIRE](#)].
- [29] M. Altenbuchinger and L.-S. Geng, *Off-shell effects on the interaction of Nambu-Goldstone bosons and D mesons*, *Phys. Rev. D* **89** (2014) 054008 [[arXiv:1310.5224](#)] [[INSPIRE](#)].
- [30] E. van Beveren and G. Rupp, *Observed $D_s(2317)$ and tentative $D(2030)$ as the charmed cousins of the light scalar nonet*, *Phys. Rev. Lett.* **91** (2003) 012003 [[hep-ph/0305035](#)] [[INSPIRE](#)].
- [31] T. Barnes, F.E. Close and H.J. Lipkin, *Implications of a DK molecule at 2.32 GeV*, *Phys. Rev. D* **68** (2003) 054006 [[hep-ph/0305025](#)] [[INSPIRE](#)].
- [32] M.A. Nowak, M. Rho and I. Zahed, *Chiral doubling of heavy light hadrons: BABAR 2317 MeV/c² and CLEO 2463-MeV/c² discoveries*, *Acta Phys. Polon. B* **35** (2004) 2377 [[hep-ph/0307102](#)] [[INSPIRE](#)].
- [33] M. Nielsen, F.S. Navarra and S.H. Lee, *New charmonium states in QCD sum rules: a concise review*, *Phys. Rept.* **497** (2010) 41 [[arXiv:0911.1958](#)] [[INSPIRE](#)].
- [34] N. Brambilla et al., *Heavy quarkonium: progress, puzzles and opportunities*, *Eur. Phys. J. C* **71** (2011) 1534 [[arXiv:1010.5827](#)] [[INSPIRE](#)].
- [35] A. Esposito, A.L. Guerrieri, F. Piccinini, A. Pilloni and A.D. Polosa, *Four-quark hadrons: an updated review*, *Int. J. Mod. Phys. A* **30** (2014) 1530002 [[arXiv:1411.5997](#)] [[INSPIRE](#)].
- [36] S. Ryan, *A study of scattering in open charm channels*, [PoS\(LATTICE2014\)114](#).

- [37] HADRON SPECTRUM collaboration, J.J. Dudek, R.G. Edwards, C.E. Thomas and D.J. Wilson, *Resonances in coupled πK - ηK scattering from quantum chromodynamics*, *Phys. Rev. Lett.* **113** (2014) 182001 [[arXiv:1406.4158](#)] [[INSPIRE](#)].
- [38] J.A. Oller and E. Oset, *N/D description of two meson amplitudes and chiral symmetry*, *Phys. Rev. D* **60** (1999) 074023 [[hep-ph/9809337](#)] [[INSPIRE](#)].
- [39] J.A. Oller and U.G. Meißner, *Chiral dynamics in the presence of bound states: kaon nucleon interactions revisited*, *Phys. Lett. B* **500** (2001) 263 [[hep-ph/0011146](#)] [[INSPIRE](#)].
- [40] N. Isgur and M.B. Wise, *Spectroscopy with heavy quark symmetry*, *Phys. Rev. Lett.* **66** (1991) 1130 [[INSPIRE](#)].
- [41] L. Castillejo, R.H. Dalitz and F.J. Dyson, *Low's scattering equation for the charged and neutral scalar theories*, *Phys. Rev.* **101** (1956) 453 [[INSPIRE](#)].
- [42] A. Martinez Torres, L.R. Dai, C. Koren, D. Jido and E. Oset, *The KD , ηD_s interaction in finite volume and the nature of the $D_s^{*0}(2317)$ resonance*, *Phys. Rev. D* **85** (2012) 014027 [[arXiv:1109.0396](#)] [[INSPIRE](#)].
- [43] H.-X. Chen and E. Oset, *$\pi\pi$ interaction in the ρ channel in finite volume*, *Phys. Rev. D* **87** (2013) 016014 [[arXiv:1202.2787](#)] [[INSPIRE](#)].
- [44] D. Zhou, E.-L. Cui, H.-X. Chen, L.-S. Geng and L.-H. Zhu, *$K\pi$ interaction in finite volume and the K^* resonance*, *Phys. Rev. D* **91** (2015) 094505 [[arXiv:1409.0178](#)] [[INSPIRE](#)].
- [45] M. Albaladejo, J.A. Oller, E. Oset, G. Rios and L. Roca, *Finite volume treatment of $\pi\pi$ scattering and limits to phase shifts extraction from lattice QCD*, *JHEP* **08** (2012) 071 [[arXiv:1205.3582](#)] [[INSPIRE](#)].
- [46] M. Albaladejo, G. Rios, J.A. Oller and L. Roca, *Finite volume treatment of $\pi\pi$ scattering in the ρ channel*, [arXiv:1307.5169](#) [[INSPIRE](#)].
- [47] F. Aceti and E. Oset, *Wave functions of composite hadron states and relationship to couplings of scattering amplitudes for general partial waves*, *Phys. Rev. D* **86** (2012) 014012 [[arXiv:1202.4607](#)] [[INSPIRE](#)].
- [48] C.W. Xiao, F. Aceti and M. Bayar, *The small $K\pi$ component in the K^* wave functions*, *Eur. Phys. J. A* **49** (2013) 22 [[arXiv:1210.7176](#)] [[INSPIRE](#)].
- [49] H. Wittig *Low-energy precision observables with $O(a)$ improved Wilson fermions*, in *Hadrons and Hadron interactions in QCD 2015 (HHIQCD2015)*, February 15–March 21, Kyoto, Japan (2015).
- [50] D.-L. Yao, M.-L. Du, F.-K. Guo and U.-G. Meißner, *One-loop analysis of the interactions between charmed mesons and Goldstone bosons*, [arXiv:1502.05981](#) [[INSPIRE](#)].